Removal of Arsenic from Simulated Groundwater by GAC-Fe: A Modeling Approach

P. Mondal, B. Mohanty, and C. B. Majumder
Dept. of Chemical Engineering, Indian Institute of Technology Roorkee, Roorkee-247667, Uttranchal, India

N. Bhandari
Dept. of Chemical Engineering and Biological Engineering, Iowa State University, Ames, IA 50011

DOI 10.1002/aic.11819

A study on kinetics and equilibrium is presented on the adsorption of arsenic species from simulated groundwater containing arsenic (As(III):As(V)::1:1), Fe and Mn in concentrations of 0.188 mg/L, 2.8 mg/L and 0.6 mg/L, respectively, by iron impregnated granular activated charcoal (GAC-Fe). Also presented is the interaction effect of As, Fe and Mn on the removal of arsenic species from water, which simulates contaminated groundwater. Among conventional models, pseudo second-order kinetic model and Freundlich isotherm were adequate to explain the kinetics and equilibrium of adsorption process, respectively. However, in comparison to conventional isotherm empirical polynomial isotherm provided a more accurate prediction on equilibrium specific uptakes of arsenic species. Effects of initial concentrations of As, Fe and Mn on the removal of total arsenic (As(T)), As(V) & As(III) have been correlated within the error limit of −0.2 to +5.64%.
AIChE J, 55: 1860–1871, 2009
Keywords: arsenic species, GAC-Fe, groundwater, adsorptive removal

Introduction

Long-term consumption of arsenic contaminated groundwater, has inflicted considerable harm on health of common people in many countries like Argentina, Bangladesh, Canada, Chile, China, Cambodia, Germany, Hungary, India, Myanmar, Mexico, Mongolia, Nepal, Pakistan, Romania, Thailand, USA, Vietnam, and so on.[1,2,3,4] Among these countries, arsenic poisoning has been observed in its most devastating form in India and Bangladesh. Considering its toxic effect on human health, the maximum contaminant level (MCL) of arsenic in drinking water has been reduced from 50 μg/L to10 μg/L by World Health Organization (WHO)[5] and United States Environmental Protection Agency (USEPA).[6] National Health and Medical Research Committee (NHMRC),[7] Australia, in 1996 had recommended MCL of arsenic in drinking water as 7 μg/L. However, for Bangladesh and India this limit is still as high as 50 μg/L.

Arsenic concentration in the groundwater of West Bengal, India, lies within 50–200 μg/l[8] and relative amounts of As(V) and As(III) in groundwater depend on the redox condition in the aquifer.[3] Recently, the relative amount of As(III) and As(V) in the groundwater of some places of West Bengal has also been reported as 1:1.[9] Among the cations present in groundwater, Fe and Mn have significant effect on the removal of arsenic species from water.[10,11] Fe and Mn are present as positively charged ions, whereas arsenic exists as negatively charged species or neutral species. Therefore, Fe and Mn are not competitors to arsenic species for adsorption onto GAC-Fe. Moreover, arsenite can be oxidized to some extent due to the presence of Fe and Mn.[10,11] Therefore, Fe, Mn and As may have some interaction effects on the removal of arsenic species.

Among the arsenic removal methods from contaminated water, the surface modified adsorbents have become more prominent in recent years.[4] Recently, several researchers

---

Correspondence concerning this article should be addressed to C. B. Majumder at chandfch@iitr.ernet.in

have reported that the iron impregnated granular activated charcoal (GAC-Fe) has very good arsenic removal capacity.[12,13,14,15,16,17,18] In these investigations a wide range of adsorbent doses and agitation periods have been undertaken and the effect of process parameters on the removal of arsenic species by GAC-Fe has been reported.

Some work has also been reported on the kinetics and equilibrium of arsenic removal from water in the absence of other metal ions using GAC-Fe.[13,17] However, there is hardly any reported work on the kinetics and equilibrium studies on arsenic removal from contaminated water by GAC-Fe in the presence of Fe and Mn, which are normally present in arsenic contaminated water.

In this work, the kinetics and equilibrium studies for the removal of arsenic species from simulated water representing contaminated groundwater in the presence of Fe and Mn have been undertaken. The interaction effects of initial concentrations of iron (Fe_o), manganese (Mn_o) and arsenic (As_o) on the removal of arsenic species have also been expressed in the form of correlations.

Models

To understand adsorption phenomena two types of models are normally developed. The first type is on the basis of agitation period (kinetics model), and the second type is on the basis of initial arsenic concentration (equilibrium model) as follows.

Kinetic models

Different kinetic models such as pseudo first-order model, pseudo second-order model, Weber and Morris model, Elovich model, etc., are normally used to describe the nonequilibrium stage of adsorption. In brief these models are described as follows.

Pseudo first-order model

Lagergren[19] showed that the rate of adsorption of pollutants on the adsorbent follows a pseudo first-order model

$$\mathrm{d}q_t/\mathrm{d}t = k_1(q_e - q_t) \tag{1}$$

where, q_e and q_t are sorption capacities (mg/g) of adsorbent at equilibrium and at a given time "t", respectively, and k_1 is the pseudo first-order adsorption rate constant (s^{-1}). Integrating and applying the boundary conditions; at $t = 0$, $q_t = 0$ and at $t = t$, $q_t = q_t$, Eq. 1 is reduced to

$$\log(q_e - q_t) = \log q_e - k_1 t/2.303 \tag{2}$$

Pseudo second-order model

Ho and McKay[20] proposed the pseudo second-order kinetic model for the adsorption process as described as follows

$$\mathrm{d}q_t/\mathrm{d}t = k_2(q_e - q_t)^2 \tag{3}$$

where, k_2 is the pseudo-second-order adsorption rate constant (g/mg s). Integrating and applying the boundary conditions; at $t = 0$, $q_t = 0$ and at $t = t$, $q_t = q_t$, Eq. 3 is reduced to

$$t/d_t = 1/(k_2 q_e^2) + t/q_e \tag{4}$$

At $t \to 0$, $k_2 q_e^2$ represents the rate of adsorption, and, hence, it is termed as initial adsorption rate h (mg/g s).

Weber and Morris model

Weber and Morris[21] described the intraparticle uptake of adsorbate during the adsorption process to be proportional to the half power of time

$$q_t = k_{id} t^{1/2} + I \tag{5}$$

where, k_{id} is intraparticle diffusion rate constant (mg $g^{-1}s^{-1/2}$), and I (mg/g) is a constant that gives indication about the thickness of the boundary layer, i.e., larger is the value of I the greater is the boundary layer effect.

Elovich model

Elovich model[22] describes the chemisorption phenomena in which desorption is negligible. In this model the rate of adsorption decreases due to the increase in surface coverage of adsorbent with time as on the following statement

$$\mathrm{d}q_t/\mathrm{dt} = \alpha \exp(-\beta q_t) \tag{6}$$

where, α is the initial adsorption rate constant (mg $g^{-1}s^{-1}$), and β is the desorption constant (g/mg). Chien and Clayton[23] simplified the aforementioned model assuming $\alpha\beta t \gg 1$, and applying the boundary conditions, at $t = 0$, $q_t = 0$ and at $t = t$, $q_t = q_t$, the model reduces to

$$q_t = \ln(\alpha\beta)/\beta + \ln(t)/\beta \tag{7}$$

Equilibrium models

The simulated ground water investigated in this work contains arsenic along with Fe and Mn. In the pH range investigated, all the metal ions except arsenic species exist as positively charged ions, where as arsenic exists as negatively charged entity. Therefore, there is no competition among the ions of metals and arsenic to occupy the same active sites on the adsorbent surface. Thus, the overall adsorption process can be modeled by monocomponent isotherms rather than multicomponent isotherms. Commonly used monocomponent isotherm models are Langmuir, Freundlich and Temkin isotherms.

The Langmuir isotherm theory is based on the assumption that adsorption is a first-order chemical process, and monolayer of adsorbed material is formed onto a series of distinct sites (unisite) on the surface of the adsorbent. Langmuir isotherm is expressed as

$$q_e = q_{\max} K_L C_e/(1 + K_L C_e) \tag{8}$$

where, $q_{\max}$ (mg/g) & K_L (l/mg) are the Langmuir constants related to the capacity and energy of adsorption, respectively.

Freundlich Isotherm is developed on the basis of the formation of monolayer due to adsorption onto a rough heterogeneous surface (multisites), and is expressed as

$$q_e = K_f C_e^{1/n} \tag{9}$$

where K_f ((mg/g)/(mg/L)$^{1/n}$), and n are Freundlich isotherm constants related to the adsorption capacity and degree of favorability of adsorption, respectively.

Temkin isotherm is derived using molecular statistical theory. It is also applicable for heterogeneous surface and can be expressed as follows

$$q_e = B_1 \ln(K_T C_e) \tag{10}$$

where K_T (l/mg) is equilibrium binding constant corresponding to the maximum binding energy and B_1 (mg/g) is related to the heat of adsorption.

To estimate the isotherm constants in Eqs. 8, 9 and 10, these equations are generally converted to their linear form as stated in Eqs. 11, 12 and 13, respectively

$$1/q_e = 1/K_L q_{\max} C + 1/q_{\max} \tag{11}$$

$$\log q_e = \log K_f + \log C_e/n \tag{12}$$

$$q_e = B_1 \ln K_T + B_1 \ln C_e \tag{13}$$

However, in the previously mentioned converted linear models the error associated with the data is not expressed properly. Hence, in recent years, the development of isotherm model in original form (i.e., q_e as a function of C_e) by regression is gradually becoming more popular as the error associated with the data is properly expressed in original form.[24] The isotherm model, in its original form, normally gives rise to polynomial equation and is termed as polynomial isotherm.[25] A polynomial isotherm of second-order is presented

$$q_e = a + cC_e - dC_e^2 \tag{14}$$

where a (mg/g), c(l/mg), and d (l^2/(g)(mg)) are constants of the polynomial isotherm. Although they provide accurate prediction, polynomial isotherm does not explain the physics of adsorption.

To examine the accuracy of fitting of experimental data by the aforementioned isotherms, Marquardt's percent standard deviation (MPSD) error function[26] was computed and is given in Eq. 15

$$MPSD = 100\sqrt{\frac{1}{(m-p)}\sum_{i=1}^{i=m}\left((q_{e,\mathrm{exp}} - q_{e,\mathrm{calc}})/q_{e,\mathrm{exp}}\right)} \tag{15}$$

The MPSD error function is similar in some respects to geometric mean error distribution modified according to the number of degrees of freedom of the system. The values of m and p in the aforementioned equations are equal to the number of experimental data points and number of parameters in the isotherm equation, respectively.

Materials and Methods

All the chemicals used in this study were of reagent grade and procured from *s.d. fine-chem* limited, India. Synthetic solutions were prepared by Milli-Q water (Q-H_2O, Millipore Corp. with resistivity of 18.2 MΩ-cm). The stock solutions containing 100 mg/L As(V) and As(III) were separately prepared by dissolving $Na_2HAsO_4.7H_2O$ and $NaAsO_2$ in water and were filtered through a 0.45 μm membrane. Granular activated charcoal (GAC), produced from wood was also procured from *s.d. fine-chem* limited. Bulk density of GAC was 40 g/100 mL.

Preparation and characterization of GAC-Fe

GAC-Fe was prepared by impregnating Fe^{3+} ions on GAC (particle size 2–4 mm) surface using ferric chloride solution containing 2.5 wt % Fe^{3+} in a similar way as described elsewhere.[12] However, in this case initial pH was adjusted to 5.8 ± 0.2 and was maintained at that level for 2 h. The pH was then raised to 8 after 2 h and then to 12 after 4 h by the addition of NaOH. Further fixation of Fe^{3+} was carried out at 70 °C on a water bath until the water evaporated completely, and then it was dried at 110 °C for 24 h. Stepwise increase in pH was done with a view to increase the chemisorption of positively charged Fe^{3+} on the GAC surface. The mechanism for Fe^{3+} impregnation on GAC surface as in the following discussion.

In the solution Fe^{3+} exists as positively charged species such as $Fe(OH)_2^+$ and $Fe(OH)^{2+}$, and as neutral species like $Fe(OH)_3$. With the increase in the value of pH the relative amounts of positively charged species decrease, and the relative amount of neutral species increase. At pH 5.8 ± 0.2, both $Fe(OH)_2^+$ and $Fe(OH)^{2+}$ coexist. However, the relative amount of $Fe(OH)^{2+}$ is more[26] than that of $Fe(OH)_2^{+\cdot}$. At pH 8 and 12 the predominating species are $Fe(OH)_2^+$ and $Fe(OH)_3$, respectively. The positively charged hydro oxides of iron can be chemisorbed on the negatively charged sites on GAC surface created by the oxides present in the ash of GAC. Furthermore, Fe^{3+} has unfilled d orbital in its electron configuration ($1s^22s^22p^63s^23p^63d^5$), and, thus, $Fe(OH)_2^+$, $Fe(OH)^{2+}$ and $Fe(OH)_3$ can make surface complexes with the carboxyl and phenolic groups present on GAC surface. Possible reactions that can take place on GAC surface leading to impregnation of Fe are[15,28,29]

$$MOH + OH^- \rightarrow MO^- + H_2O\,(\text{at a pH above the pH}_{zPC}\ \text{of MOH})$$

$$MO^- + Fe(OH)_2^+ \rightarrow (MO) - Fe(OH)_2$$

$$2MO^- + Fe(OH)^{2+} \rightarrow (MO)_2 - Fe(OH)$$

$$2(C{-}XH) + Fe(OH)_2^+ \rightarrow (C{-}X)_2 - Fe(OH)_2^+ + 2H^+$$

$$2(C{-}XH) + Fe(OH)^{2+} \rightarrow (C{-}X)_2 - Fe(OH)^{2+} + 2H^+$$

$$2(C{-}XH) + Fe(OH)_3 \rightarrow (C{-}X)_2 - Fe(OH)_3^+ + 2H^+$$

where, group (C—X) represents (C—COO) and (C—O) groups generated due to the carboxyl and phenolic groups present on GAC surface, respectively. MOH represents the oxides of Si, Al, Fe, Ca and Mg present in the ash of GAC. The pH_{zpc} values for the oxides of Si, Al, Fe, Ca and Mg are 2.2, 8, 8.3,

Table 1. Properties of GAC-Fe

Adsorbent	Particle size (mm)	Elemental analysis (%)	Proximate analysis (%)	BET Surface area (m^2/g)	Pore volume (cm^3/g)	Bulk density (g/l)	Impg Fe content (wt. %)
GAC-Fe	2–4	C : 74.39 H : 1.57 N : 0.30 S : 0.15 Others: 23.59	Ash : 8.93 M: 8.85 Others: 82.22	488.24	mi: 0.1746 me:0.0212 ma:0.0020	658.01	4.78
GAC	2–4	C : 75.06 H : 1.90 N : 0.00 S : 0.00 Others: 23.04	Ash : 2.58 M: 9.71 Others: 87.71	583.23	mi: 0.2044 me:0.0495 ma:0.0036	605.02	–

Impg Fe: impregnated Fe; M: moisture; mi: micro pore (dia < 2 nm), me: meso pore (dia 2–50 nm),; ma: macro pore(dia > 50 nm).

11 and 12.4, respectively. Therefore, oxides of Fe, Ca, Si and Al present on the surface of GAC as hydroxides can adsorb $Fe(OH)_2^+$ and $Fe(OH)^{2+}$. However, the same is not true for Mg as the maximum pH for impregnation of Fe (pH 12) is less than the pH_{zpc} of MgO (pH 12.4). Key properties of untreated GAC and GAC-Fe are shown in Table 1.

Elemental analysis of GAC-Fe and GAC was carried out by an elemental analyzer system (Elementar Analysensysteme GmbH, model Vario-EL V3.00), and bulk density was measured by a picnometer. Surface area and pore volume of the samples were measured by N_2 adsorption isotherm using an ASAP 2010 micromeritics instrument by Brunauer-Emmett-Teller (BET) method, and using the software of micromeritics. Nitrogen was used as cold bath (77.15 K). SEM photograph was taken by an electron microscope (LEO Electron Microscopy, Ltd., U.K).

Procedure

For kinetics study each 50 mL of the synthetic water sample containing 188 μg/L As(T) (in the ratio As(III):As(V) :: 1:1), 2.8 mg/L Fe and 0.6 mg/L Mn was added with 0.25 g GAC-Fe in a 100 mL vessel. Agitation period was varied from 30 min to 32 h with a speed of 180 rpm. Temperature was maintained at 29 ± 1°C. The solution pH was maintained at 7.1 ± 0.1 by measuring it intermittently each 2 h, and controlled by dropwise addition of N/10 HNO_3 whenever required. In each case, after the adsorption was over, the solution was filtered through a 0.45 μm membrane filter.

The filtrate was analyzed for total arsenic present in the solution by a PerkinElmer ICP-MS model ELAN-DRC-e. Arsenic speciation was done by Edward's ion exchange method using strong base anion resin AGX8, with correction due to the presence of Fe and Mn ions as described elsewhere.[30] Analysis of Fe and Mn was done by atomic absorption spectroscopy AAS, GBC, Avanta, Australia. All the experiments were repeated thrice and average results were reported.

For equilibrium study, five different experiments were carried out, each with an agitation period of 42 h based on earlier observations, and for these experiments the values of As_o was varied in five steps from 0.188, 0.333, 0.407, 2.20 and 3.17 mg/L. Temperature and pH of the solution were kept constant similar to the aforementioned described kinetics studies.

To study the interaction effects of As_o, Fe_o and Mn_o, on the removal of arsenic species, a full factorial design with three different factors was carried out. The first factor was initial concentration of As (As_o) at four levels and these were 0.167, 0.333, 0.5 and 2 mg/L. The other two factors were initial Fe and Mn concentration (Fe_o and Mn_o) and three levels of Fe_o and Mn_o were studied. Three levels of Fe were 2.7, 1.8 & 0.9 mg/L and for Mn these values were 0.2, 0.4 and 0.6 mg/L. The full design with all 36 experiments is given in Table 2 in terms of coded values. Agitation time and pH were kept at 24 h and 7.1 ± 0.1, respectively.

Results and Discussion

Adsorption kinetics, adsorption equilibrium and interaction effects of Fe_o, Mn_o, and As_o on the removal of arsenic species by the adsorption on GAC-Fe are discussed as follows.

Adsorption kinetics

To study the kinetics of adsorption of arsenic species on GAC-Fe, specific uptake of various arsenic species with agitation time is plotted in Figure 1. From Figure 1 it is evident that adsorption of arsenic takes place with a very fast initial stage followed by a plateau stage. This phenomenon can be explained on the basis of mechanism of adsorption supplemented with hydrodynamics of the system. In the beginning, both the number of available active sites on GAC-Fe surface for adsorption and the concentration of arsenic species in the solution are maximum, thus, maximum driving force for adsorption of arsenic is present. To supplement the adsorption, agitation provides the energy required for arsenic species to transport itself from the bulk of the solution to the active sites of the adsorbent, thereby reducing the resistance to mass transfer between the bulk phase and adsorbent. In fact, all the aforementioned three facts, i.e., the presence of large number of active sites, higher driving force and reduction of resistance to mass transfer by agitation promote adsorption. With the increase in agitation period, more and more arsenic species get the opportunity to come in contact with the GAC-Fe surface. Hence, at the initial stage, rate of % removal of arsenic species is high with the increase in agitation period. However, after certain value of agitation period (>10 h) the rate of % removal of arsenic species decreases considerably and finally becomes zero, indicated

Table 2. Design of Experiments for Determining Interaction Effects of Fe_o, Mn_o and As_o on Arsenic Removal (for As_o : 1 = 0.167 mg/L, 2 = 0.333 mg/L, 3 = 0.5 mg/L and 4 = 2 mg/L; for Fe_o: 1 = 0.9 mg/L, 2 = 1.8 mg/L and 3 = 2.7 mg/L; for Mn_o: 1 = 0.2 mg/L, 2 = 0.4 mg/L and 3 = 0.6 mg/L)

Run	As_o	Fe_o	Mn_o
1	3	3	1
2	3	2	2
3	2	1	1
4	1	2	3
5	4	2	3
6	3	3	2
7	1	2	1
8	3	1	2
9	4	2	2
10	4	2	1
11	3	1	3
12	3	2	1
13	2	2	1
14	4	3	2
15	3	2	3
16	3	1	1
17	4	3	3
18	2	2	3
19	4	3	1
20	2	1	3
21	4	1	3
22	3	3	3
23	2	3	1
24	1	3	3
25	4	1	1
26	2	3	3
27	1	3	2
28	4	1	2
29	2	2	2
30	2	3	2
31	1	2	2
32	1	1	1
33	1	1	3
34	1	1	2
35	2	1	2
36	1	3	1

by the fact that specific uptake becomes constant. The possible reasons for this are given next.

At the experimental pH (7.1 ± 0.1), As(V) exists in solution as negatively charged species as $H_2AsO_4^-$ and As(III) exists predominantly as neutral species, but its presence as negatively charged species in small amounts cannot be ruled out. In addition to it a small amount of As(III) is also oxidized to As(V) as $H_2AsO_4^-$ in the presence of Fe and Mn. Negatively charged As(V), As(III) and converted As(V) from As(III) can be chemisorbed on the predominantly positively charged surface of GAC-Fe, which is created due to the impregnation of Fe^{3+} ion on GAC surface as discussed elsewhere.[18] Neutral arsenic species (As(III)), to some extent can also be adsorbed by physical adsorption. During the adsorption process some amount of negatively charged arsenic species can also be attached to surface complexes produced on the GAC-Fe surface through the exchange of hydroxyl ions of these surface complexes. Possible reactions for the adsorption/attachment of arsenic species on GAC-Fe are as follows[31,15,29]

$$(\mathrm{M{-}O}) - \mathrm{Fe(OH_2^+)_2} + \mathrm{HAsO_4^{2-}} \rightarrow (\mathrm{M{-}O}) - \mathrm{Fe(HAsO_4)} + 2\mathrm{H_2O}$$

$$(\mathrm{M{-}O})_2 - \mathrm{Fe(OH_2^+)} + \mathrm{H_2AsO_4^-} \rightarrow (\mathrm{M{-}O})_2 - \mathrm{Fe(H_2AsO_4)} + \mathrm{H_2O}$$

$$(\mathrm{C{-}X})_2 - \mathrm{Fe(OH)^{2+}} + \mathrm{HAsO_4^{2-}} \rightarrow (\mathrm{C{-}X})_2 - \mathrm{Fe(AsO_4)} + \mathrm{H_2O}$$

$$(\mathrm{C{-}X})_2 - \mathrm{Fe(OH)_2^+} + \mathrm{H_2AsO_4^-} \rightarrow (\mathrm{C{-}X})_2 - \mathrm{Fe(OH)HAsO_4} + \mathrm{H_2O}$$

$$(\mathrm{C{-}X})_2 - \mathrm{Fe(OH)_3^o} + \mathrm{H_2AsO_4^-} \rightarrow (\mathrm{C{-}X})_2 - \mathrm{Fe(OH)_2H_2AsO_4} + \mathrm{OH^-}$$

$$(\mathrm{C{-}X})_2 - \mathrm{Fe(OH)_2^+} + \mathrm{H_2AsO_3^-} \rightarrow (\mathrm{C{-}X})_2 - \mathrm{Fe(OH)HAsO_3} + \mathrm{H_2O}$$

$$(\mathrm{C{-}X})_2 - \mathrm{Fe(OH)_3^o} + \mathrm{H_2AsO_3^-} \rightarrow (\mathrm{C{-}X})_2 - \mathrm{Fe(OH)_2H_2AsO_3} + \mathrm{OH^-}$$

Presence of FeOOH group on GAC-Fe has been identified with the help of XRD analysis of GAC-Fe.[12] The adsorption/attachment, of arsenic species, as negatively charged species along with some neutral species, has also been confirmed by comparing FTIR spectra of GAC-Fe before and after adsorption of arsenic.[12]

Within a few hours of agitation most of the negatively charged arsenic species are chemisorbed on GAC-Fe surface, as a result, most of the active sites are occupied and the concentration of arsenic species in the solution reduces. Thus, the driving force, as well as active site density both decreases considerably (resistance due to mass transfer remains constant), leading to a slow rate of adsorption proceeding toward zero rate. Hence, despite similar intensity of agitation more time is required for the adsorption of arsenic species.

To estimate the kinetic parameters attached to different kinetic models, the models were regressed with the help of data obtained in this investigation as described in the Models section, and are reported in Table 3. Out of the four models tested and reported in Table 3, the value of correlation coefficient (R^2) for pseudo second-order model is highest, and,

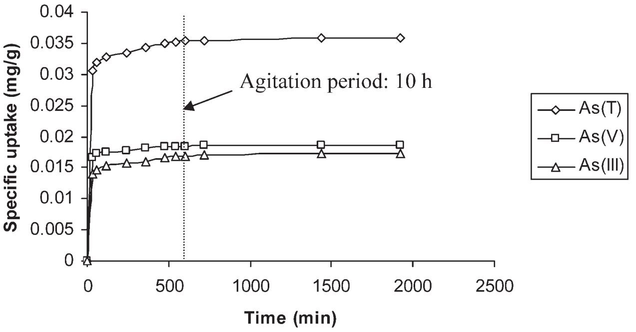

Figure 1. Removal of arsenic species with agitation time (Process conditions: pH: 7.1 ± 0.1, temperature: 29 ± 1 °C, particle size : 2–4 mm, adsorbent concentration: 5 g/L, As(T): 188 μg/L (As(III): As(V)::1:1), Fe_o: 2.8 mg/L, Mn_o: 0.6 mg/L).

Table 3. Kinetic Parameters of Various Kinetic Models for Adsorption of Arsenic Species on GAC-Fe

Model	R^2	$q_{ecal.}$	$q_{eexp.}$	Kinetic parameters
As(T)				
Pseudo First order	0.90	0.08518	0.03609	$K_1(s^{-1})$: 3.07×10^{-5}
Pseudo Second order	0.99	0.03604	0.03609	$K_2(g(mg)^{-1}s^{-1})$: 0.0425
Intra particle diffusion model	0.79	–	–	$K_{id}(mg(g)^{-1}s^{1/2})$: 7.74×10^{-4} $I(mg(g)^{-1})$: 0.03
Elovich model	0.94	–	–	$\alpha(mg(g)^{-1}s^{1/2})$: 6.64×10^{6} $\beta(g(mg)^{-1})$: 769.23
As(V)				
Pseudo First order	0.87	0.052692	0.018766	$K_1(s^{-1})$: 2.33×10^{-5}
Pseudo Second order	1.0	0.018650	0.018766	$K_2(g(mg)^{-1}s^{-1})$: 0.1383
Intra particle diffusion model	0.73	–	–	$K_{id}(mg(g)^{-1}s^{1/2})$: 3.87×10^{-4} $I(mg(g)^{-1})$: 0.017
Elovich model	0.93	–	–	$\alpha(mg(g)^{-1}s^{1/2})$: 6.17×10^{10} $\beta(g(mg)^{-1})$: 2000
As(III)				
Pseudo First order	0.97	0.075276	0.017322	$K_1(s^{-1})$: 4.22×10^{-5}
Pseudo Second order	1.0	0.017393	0.017322	$K_2(g(mg)^{-1}s^{-1})$: 0.0602
Intra particle diffusion model	0.79	–	–	$K_{id}(mg(g)^{-1}s^{1/2})$: 7.74×10^{-4} $I(mg(g)^{-1})$: 0.031
Elovich model	0.97	–	–	$\alpha(mg(g)^{-1}s^{1/2})$: 7452.27 $\beta(g(mg)^{-1})$: 1250

thus, predicts the value of $q_{epredict}$ best. Predicted specific uptake value of As(T), obtained from pseudo second-order model shows an error of only 0.1%.

In an adsorption process the adsorbate is first transported from bulk of the solution to the surface of adsorbent. Then it is either gets adsorbed on the active sites available on the outer surface of adsorbent or diffuses into the interior part of the adsorbent through pore diffusion (intraparticle diffusion), and gets adsorbed on the active sites available on the pore surface. Hence, the overall adsorption process is controlled by either or in combination of film diffusion (external mass-transfer effect), pore diffusion (intraparticle mass-transfer effect), and intrinsic adsorption[32] (physical adsorption/chemical adsorption/attachment through hydroxyl ion exchange, etc).

To investigate the possibilities of pore diffusion (intraparticle diffusion) for the adsorption of arsenic species, as well as to understand the implication of data for improved adsorbent and process design, q_t vs. $t^{1/2}$ plots have been developed for As(III) and As(V) as shown in Figure 2. From Figure 2 it is evident that the q_t vs. $t^{1/2}$ plots exhibit multilinearity (having three linear parts), which indicates that the pore diffusion does not solely control the adsorption process for both As(III) and As(V).[33] The most steeper parts (P_1 and P'_1) at the initial stage of adsorption, for both As(III) and As(V), are due to the instantaneous utilization of the most readily available adsorbing sites on the adsorbent surface. P_1 and P'_1 are usually attributed to boundary layer diffusion or external mass-transfer effects.[34]

It is interesting to note that the spread of zone P'_1 is more than P_1, which indicates that rate of bulk diffusion for As(V) is faster than that of As(III). This might be due to the fact that majority of As(III) exists as neutral species, whereas As(V) exists as negatively charged species, and, thus, As(V) experiences more attraction forces toward positively charged sites on the GAC-Fe surface. This in turn neutralizes to some extent, external mass-transfer resistance offered by the media for the transport of As(V) ion than As(III), and results in more adsorption of As(V) than As(III). Due to this reason, in normal practices, As(III) is oxidized to As(V) before adsorption for getting more arsenic adsorption. The lower value of "I" predicted by intraparticle diffusion model for As(V) (0.017 mg/g) than that of As(III) (0.031 mg/g), also supports that As(III) experiences more external mass-transfer resistance for being shifted from bulk of the solution to the adsorbent surface than As(V).

In Figure 2, straight portions P_2 and P'_2 depict macropore diffusion, whereas P_3 and P'_3 depict micropore/mesopore diffusion.[34] From Figure 2 it is evident that arsenic species adsorbed through macropore diffusion is more than that through micropore/mesopore diffusion for both As(III) and As(V). This can be explained as follows.

In GAC-Fe, the pore volumes for micropore (<2 nm), mesopore (2 to 50 nm), and macropore (>50 nm) are 0.1746 cm^3/g, 0.0212 cm^3/g and 0.0020 cm^3/g, respectively. Whereas, the average size of As(V) and As(III) are 41nm and 48 nm, respectively.[13] Hence, due to lesser size of micropores than that of arsenic species, the adsorption of arsenic species through micropore diffusion is not possible.

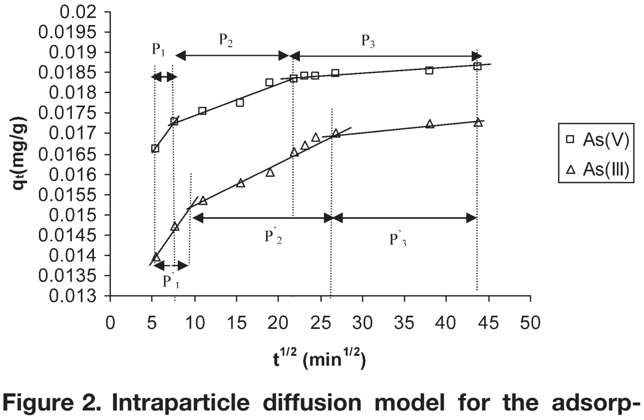

Figure 2. Intraparticle diffusion model for the adsorption of various arsenic species using GAC-Fe.

Furthermore, as the diameter of the pore should be at least more than twice the diameter of ion for proper adsorption inside the pore, adsorption on mesopore is also unlikely. Hence, despite having more micropore/mesopore volume in GAC-Fe, adsorption of arsenic species through micropore/mesopore diffusion is also negligible, as evident in Figure 2. However, due to bigger size of macropores the adsorption of arsenic species through macropore diffusion is considerable. If we compare the pore volumes of GAC-Fe with that of untreated GAC it seems that the macropore, mesopore and micropore volumes of GAC (0.0036, 0.0495 and 0.2044 cm^3/g, respectively) are reduced by 44.4%, 57.1% and 14.6% receptively, due to the impregnation of Fe^{3+} on GAC. Therefore, an adsorbent having more macropore volume will be more efficient for surface modification, consequently will assist removal of arsenic.

To find out the rate limiting step of the overall adsorption process the values of first-order rate constant (K_1) of As(III) and As(V), obtained from the slopes of the straight lines of first-order model and reported in Table 2, have been utilized. The pore diffusion coefficients and film diffusion coefficients for both As(III) and As(V) have been computed[35] from Eqs. 16 and 17

$$t_{(1/2)} = 0.030r^2/D_p \qquad (16)$$

$$t_{(1/2)} = 0.230r\delta/D_f \times (C_o/C_e) \qquad (17)$$

Equations 16 and 17 are called half time equations where r is the radius of the adsorbent in cm, δ is the thickness of the water film adhered to the adsorbent in cm, D_p and D_f are pore and film diffusion coefficient, respectively in cm^2/s. C_o and C_e are the concentration of arsenic species on the adsorbent and in the solution at equilibrium, respectively. $t_{(1/2)}$ is the time required to bring down the arsenic concentration to half the initial concentration in seconds. $t_{(1/2)}$ has been calculated[35] from Eq. 18

$$t_{(1/2)} = -[\ln(0.5)]/K_1 \qquad (18)$$

Values of $t_{(1/2)}$ obtained from Eq. 18 for both As(III) and As(V) have been substituted in Eqs. 16 and 17 to obtain the values of D_p and D_f assuming δ value as 0.001 cm.[35]

The values of D_p and D_f for As(III) are 4.11×10^{-6} cm^2/s and 2.46×10^{-7} cm^2/s, respectively. Similarly, for As(V) these values are 2.27×10^{-6} cm^2/s and 5.44×10^{-6} cm^2/s, respectively. According to Michelson et al[36] if film diffusion is the rate limiting step the value of D_f should be between 10^{-6} and 10^{-8} cm^2/s, but on the other hand, if the pore diffusion is in the rate limiting step, the D_p value should be in the range of 10^{-11} and 10^{-13} cm^2/s for heavy metals.[36] Therefore, in this case pore diffusion is not the rate limiting step for both As(III) and As(V). This fact is also supported by the R^2 value (0.79) of the Weber Morris model as shown in Table 3.

For As(III), the D_f value (2.46×10^{-7} cm^2/s) lies between 10^{-6} and 10^{-8} cm^2/s, and for As(V) the D_f value (5.44×10^{-6} cm^2/s) is also in the order of 10^{-6}. Therefore, it seems that the film diffusion is the rate limiting step for both As(III) and As(V). Larger D_f and lower D_p value of As(V) than that of As(III) is due to the existence of As(V) as completely positively charged moiety, and As(III) as predominantly neutral moiety at the experimental pH. Due to negative charge of As(V) it is easily transported from the bulk of the solution to the predominantly positively charged surface of the adsorbent and gets adsorbed on the active sites of adsorbent surface rather than the interior pores.

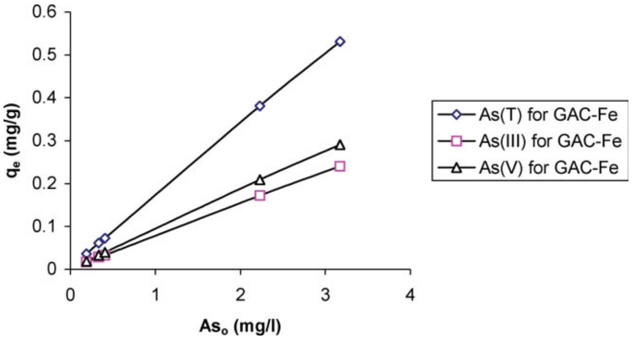

Figure 3. Change of equilibrium specific uptake with increasing As_o (Process conditions: pH: 7.1 ± 0.1, temperature: 29 ± 1 °C, agitation period: 42 h, particle size : 2–4 mm, adsorbent concentration: 5 g/L, As(T): 188 μg/L (As(III): As(V)::1:1), Fe_o: 2.8 mg/L, Mn_o: 0.6 mg/L).

[Color figure can be viewed in the online issue, which is available at www.interscience.wiley.com.]

Adsorption equilibrium

To study the state of equilibrium during adsorption of arsenic species on GAC-Fe surface, experiments have been conducted with As_o values of 0.188, 0.333, 0.407, 2.20 and 3.17 mg/L. The specific uptake values at equilibrium for As(T), As(V) and As(III) at various As_o values are shown in Figure 3, which shows that specific uptake increases with increase in the value of As_o. The possible explanation can be given with the help of surface charge on GAC-Fe surface at the pH value of experiment (7.1 ± 0.1), and the nature of charges on As(III) and As(V) ions. At pH value of 7.1 ± 0.1, GAC-Fe surface contains predominantly positive charges. Therefore, with the increase in arsenic concentration in the solution the driving force for adsorption of negatively charged arsenic species on the positively charged sites of GAC-Fe surface increases, leading to an increased adsorption of arsenic species on the GAC-Fe surface. The linear nature of the specific uptake vs. As_o plots, as shown in Figure 3 indicates that many positive sites on GAC-Fe surface remain unoccupied, which is also evident by comparing the SEM of GAC-Fe before and after adsorption/attachment of arsenic as shown in Figure 4a and b.

To determine the equilibrium parameters for the adsorption of arsenic species on GAC-Fe surface, experimental data were used to fit different adsorption isotherms as reported in the Models section. Isotherm constants, R^2 and MPSD values of these isotherm models are summarized in

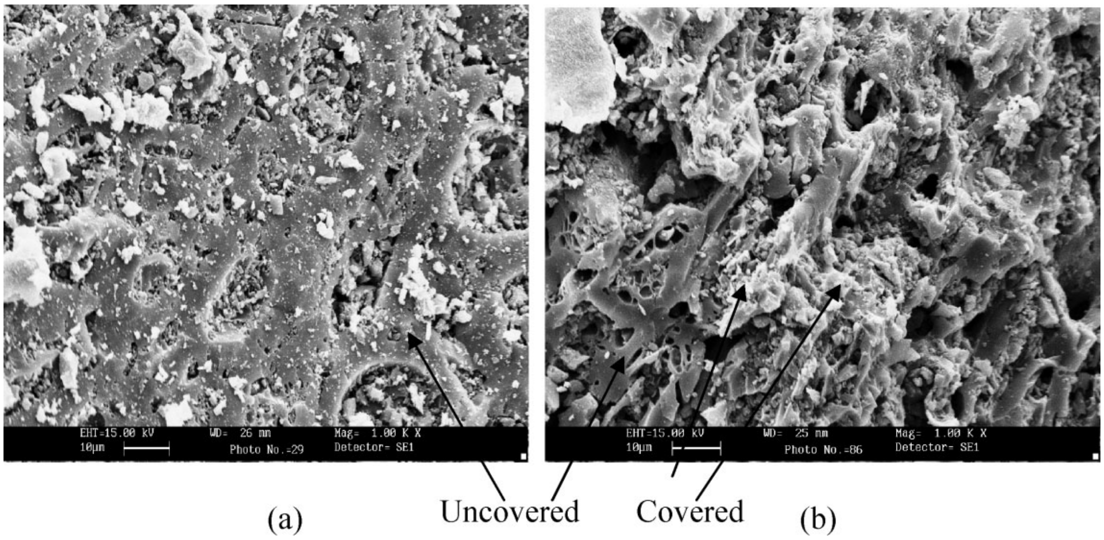

Figure 4. SEM of GAC-Fe (a) GAC-Fe before adsorption, and (b) GAC-Fe after adsorption (magnification 1.0 KX).

Table 4. From Table 4 it is evident that MPSD is minimum when the quadratic polynomial isotherm is used, indicating that it gives a more accurate prediction about the specific uptake value than any other isotherms, such as Freundlich, Langmuir or Temkin isotherms.

Polynomial isotherm constants are determined by the regression of a quadratic polynomial equation correlating specific uptake and equilibrium arsenic concentration. However, to find out the isotherm constants of Langmuir, Freundlich and Temkin isotherms the original forms of these isotherms are converted to linear forms as described in the Models section. The slope and intercepts of these derived linear forms of the isotherms are used to determine the isotherm constants. The error associated with the fitting of experimental data is properly expressed in a better way in polynomial isotherm (isotherm in original form) than the other isotherms (isotherms in derived forms). Consequently, the prediction of specific uptake by polynomial isotherm is more

Table 4. Equilibrium Constants and MPSD Values of Various Isotherm Models for the Adsorption of Arsenic Species on GAC-Fe (As_o value: 0.188 to 0.317 mg/l)

Model	R^2	Isotherm constants	MPSD
For As(T)			
Langmuir isotherm	0.9	K_L(l/mg): 19.46275 q_{max}(mg/g): 0.235154	21.3528
Freundlich isotherm	0.9841	K_f(l/mg): 0.787179 n : 1.449275	6.467253
Temkin isotherm	0.9053	B(mg/g): 0.1252 K_T(l/mg): 79.4715	47.43715
Quadratic polynomial isotherm	0.998	a(mg/g): 0.0232961 c((l/mg): 1.2824 d((l^2/(g)(mg):- 0.58252	2.454306
For As(V)			
Langmuir isotherm	0.9329	K_L(l/mg): 102.5861 q_{max}(mg/g): 0.153995	32.13612
Freundlich isotherm	0.9838	K_f(l/mg): 0.93342 n : 1.707067	16.38709
Temkin isotherm	0.9355	B(mg/g): 0.0583 K_T(l/mg): 663.4325	69.5421
Quadratic polynomial isotherm	0.999	a(mg/g): 0.0118165 c((l/mg): 0.710453 d((l^2/(g)(mg):- 0.33244	3.779037
For As(III)			
Langmuir isotherm	0.8702	K_L(l/mg): 25.86536 q_{max}(mg/g): 0.097116	20.09119
Freundlich isotherm	0.9759	K_f(l/mg): 0.430116 n : 1.421666	6.395897
Temkin isotherm	0.8914	B(mg/g): 0.0584 K_T(l/mg): 91.88593	45.68459
Quadratic polynomial isotherm	0.999	a(mg/g): 0.0106607 c((l/mg): 0.690334 d((l^2/(g)(mg):- 0.23723	2.515796

accurate than other isotherms.[24] However, the polynomial form is purely empirical in nature, and lacks physical interpretation, and it cannot offer insight required to understand the mechanism of arsenic adsorption.

Among the conventional isotherms, the Freundlich isotherm provides the best prediction of specific uptake followed by Langmuir and Temkin for both arsenic species investigated. In GAC-Fe, positive charges are created on its surface by chemisorption, as well as surface complexion reactions as discussed elsewhere,[12,18] and, thus, it provides multisites for adsorption. Due to the aforementioned fact, Freundlich isotherm provides better prediction for the specific uptake of arsenic species. Recently, Freundlich isotherm has also been found more suitable to explain the adsorption equilibrium for the adsorption of arsenic species on $FeCl_3$ treated tea fungal biomass,[37] granular ferric hydroxide,[38] and iron oxide coated sand.[39]

The $q_{\max}$ value obtained from Langmuir isotherm for the As(T) adsorption using GAC-Fe is 235 μg/g, and the equilibrium arsenic concentration in treated water (7.6 μg/L) is less than the MCL value for arsenic in drinking water as per WHO standard (10 μg/L). Furthermore, it is a well known fact that in a batch rector with stirring (stirred-tank/slurry reactor configuration), the adsorption equilibrium reaches against lower adsorbate (effluent from the process) concentration, resulting in low adsorption capacity of the adsorbent. Hence, batch operation gives conservative results. On the contrary, in fixed-bed configuration, the equilibrium reaches against adsorbate concentration in influent, and maximum loading capacity of the adsorbent is obtained. Maji et al.[35] have compared the batch and column operation for the treatment of real-life ground water containing 330 μg/L arsenic using laterite soil.[35] They have shown that the specific uptake for arsenic adsorption on laterite soil in fixed-bed configuration is 27.9 μg/g, which is ~72% more than the specific obtained in batch operation (16.2 μg/g). In this study, the specific uptake for the adsorption of As(T) by GAC-Fe in batch operation is 35.8 μg/g, which is more than double of the specific uptake of the adsorbent used by Maji et al.[35] Therefore, it seems that this adsorbent (GAC-Fe) is superior to the recently reported laterite soil,[35] and it is expected that the specific uptake for the adsorption of As(T) in fixed-bed configuration using GAC-Fe will be much more than 35.8 μg/g.

Majhi et al. 2008 have also found that using laterite soil in continuous reactor, ~100 bed volume of water containing 330 μg/L of arsenic can be treated until the arsenic concentration in treated water remains below 9 μg/L. In this study, the initial arsenic concentration is ~57% of the initial arsenic concentration used by Maji et al.[35] and the specific uptake for As(T) adsorption on GAC-Fe, in batch reactor, is more than double of the specific uptake for As(T) adsorption on laterite soil as discussed earlier. Furthermore, from the first part of this section it appears that after adsorption of arsenic on GAC-Fe under the experimental conditions many active sites remain unoccupied on GAC-Fe. Therefore, it seems that this adsorbent can be able to treat much more bed volume ($\gg$100 bed volume) of water in continuous operation than the adsorbent used by Maji et al.[35] However, more investigation is required to get the actual data to scale-up this process.

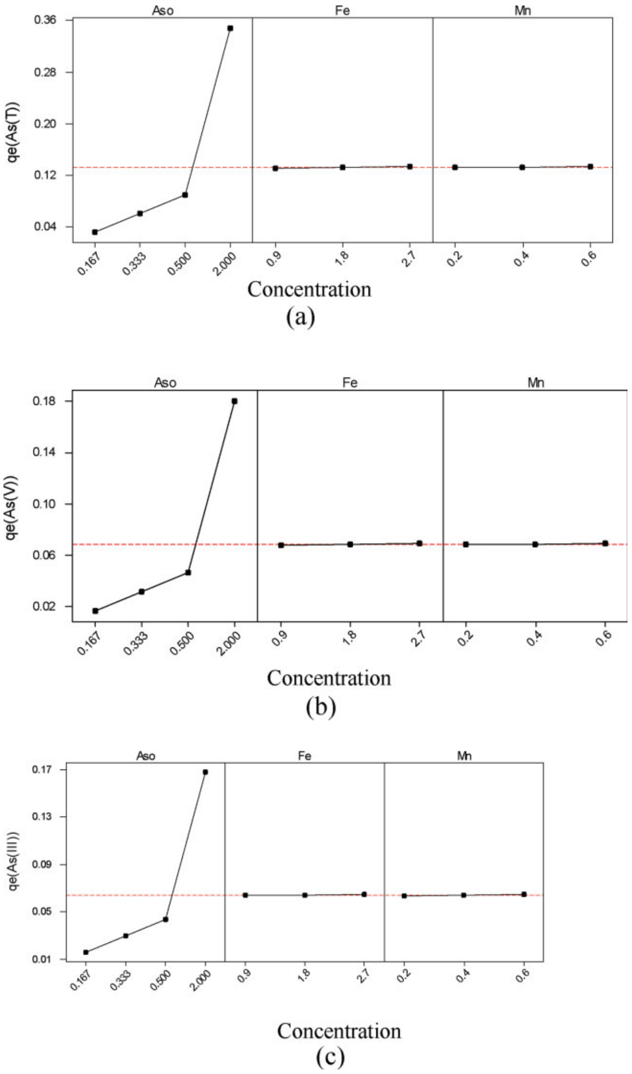

Figure 5. Main effects of As_o, Fe_o and Mn_o on the removal of As(T), As(III) and As(V) (a) for As(T), (b) for As(V), and (c) for As(III).

[Color figure can be viewed in the online issue, which is available at www.interscience.wiley.com.]

Effect of interaction among As_o, Fe_o and Mn_o on the removal of arsenic species

To study the interaction effects of As_o, Fe_o and Mn_o on the removal of As(T), As(V) and As(III) from simulated ground water, experiments have been conducted in batch reactor as described in the Procedure section. The output data have been analyzed with the help of Minitab software to get the main effects of As_o, Fe_o and Mn_o on the removal of As(T), As(V) and As(III) as shown in Figure 5a,b and c, respectively.

Figure 5a,b and c show that specific uptakes of As(T), As(V) and As(III) increase considerably with the increase in As_o. However, the increase in specific uptake of As(T), As(V) and As(III) with the increase in Fe_o and Mn_o are not significant. With increase in As_o, the driving force for adsorption increases as the GAC-Fe surface is predominantly positively charged, and arsenic species is also predominantly

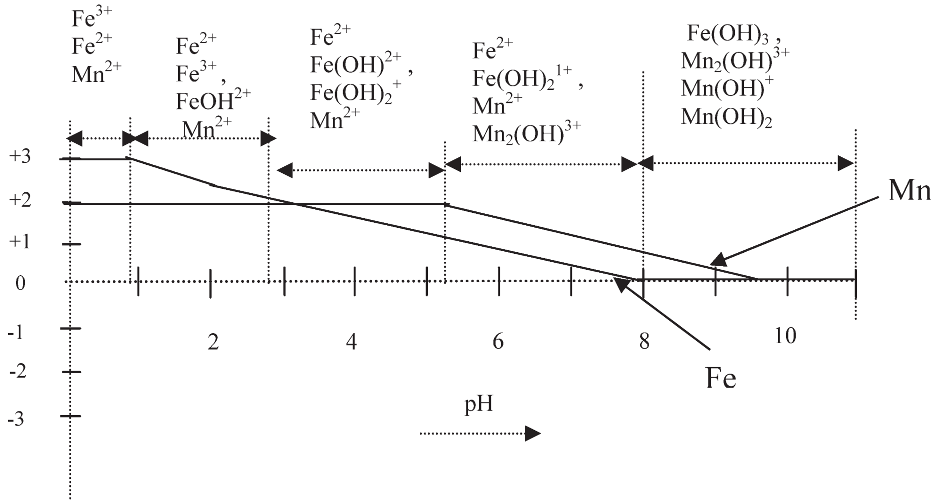

Figure 6. Change of ionic character of iron and manganese with change in solution pH.

negatively charged under present experimental conditions. Furthermore, a considerable amount of active sites on the surface of GAC-Fe also remain unoccupied even after the adsorption process, as evident from the straight curves in Figure 3, and discussed in the Adsorption equilibrium section. Due to these reasons specific uptake for the adsorption of As(T), As(V) and As(III) increases considerably with the increase in As_o.

With the increase in Fe_o and Mn_o in the solution, a number of positively charged sites created on the surface of GAC-Fe after their adsorption, increases. However, the effects of the increase in Fe_o and Mn_o are not significant when the data is presented in terms of specific uptake as shown in Figure 5b and c, respectively. Only a slight increase in arsenic removal becomes visible when the data is presented in terms of % removal. The increase in % removal of As(V) and As(III) due to the increase in Fe from 0.9 mg/L to 2.7 mg/L, at constant As_o(0.167 mg/L) and Mn_o (0.6 mg/L), are 1.84% and 1.04%, respectively. Similarly, the increase in % removal of As(V) and As(III) due to the increases in Mn from 0.2 mg/L to 0.6 mg/L, at constant As_o(0.167 mg/L) and Fe_o (2.7 mg/L), are 5.0% and 3.73%, respectively. The aforementioned observations are attributed to the very low arsenic concentration in the solution.

Regression equations correlating As_o, Fe_o and Mn_o, with specific uptake of As(T), As(V) and As(III), have been obtained using Sigma plot software with 95% confidence, and are expressed through Eqs. 19, 20 and 21, respectively

$$\begin{aligned} q_{\mathrm{As(T)}} = {} & 0.172 \times As_o + 0.0013 \times Fe_o + 0.0084 \times Mn_o \\ & - 0.0003 \times Fe_o \times Mn_o - 0.0029 \times As_o \times Fe_o - 0.0056 \\ & \times As_o \times Mn_o + 0.0048 \times As_o \times Fe_o \times Mn_o \\ R^2 = {} & 0.99 \end{aligned} \tag{19}$$

$$\begin{aligned} q_{\mathrm{As(V)}} = {} & 0.0893 \times As_o + 0.0007 \times Fe_o + 0.0044 \times Mn_o \\ & - 0.0002 \times Fe_o \times Mn_o - 0.0018 \times As_o \times Fe_o \\ & - 0.0046 \times As_o \times Mn_o + 0.0032 \times As_o \times Fe_o \times Mn_o \\ R^2 = {} & 0.99 \end{aligned} \tag{20}$$

$$\begin{aligned} q_{\mathrm{As(III)}} = {} & 0.0827 \times As_o + 0.0006 \times Fe_o + 0.0040 \times Mn_o \\ & - 0.0001 \times Fe_o \times Mn_o - 0.0011 \times As_o \times Fe_o \\ & - 0.0009 \times As_o \times Mn_o + 0.0015 \times As_o \times Fe_o \times Mn_o \\ R^2 = {} & 0.99 \end{aligned} \tag{21}$$

where, $q_{\mathrm{As(T)}}$, $q_{\mathrm{As(V)}}$ and $q_{\mathrm{As(III)}}$ are specific uptakes for the removal of As(T), As(V) and As(III), respectively. From the analysis of variance (ANOVA) of the aforementioned correlations it has been observed that the *F* values for Eqs. 19, 20 and 21 are 76044, 34574 and 49329, respectively, whereas the *p* value < 0.0001 for all the aforementioned correlations. This indicates the suitability of these equations under the domain of the present experimental conditions. The aforementioned equations show that the values of coefficients attached to Mn_o are greater than those of Fe_o, indicating that the effect of Mn_o on the removal of arsenic species is more than that of Fe_o. This fact can be explained as follows.

In the experimental pH (7.1 ± 0.1), Mn exists predominantly as Mn^{2+} ($Mn(H_2O)_6^{2+}$), whereas Fe predominantly exists as $Fe(OH)_2^+$ in the solution as shown in Figure 6.[27,40,41,42] Hence, after their attachment to the phenolic, as well as carboxyl groups present on GAC-Fe surface, Mn creates positive sites with double charge, whereas, Fe creates it with single charge. Thus, the Mn^{2+} ion attached to the surface of GAC-Fe would adsorb more negatively charged arsenic species than Fe. As a result, the effect of Mn_o on the removal of arsenic species is more than that of Fe_o.

The second-order interaction coefficients for Fe_o and Mn_o, As_o and Fe_o and As_o and Mn_o are negative, whereas it is positive for third-order interaction. The reason for this fact is not clear.

The predicted specific uptake values, computed using Eq. 19 to Eq. 21, for the adsorption of As(T), As(V) and As(III) on GAC-Fe under experimental conditions are plotted against theoretical specific uptakes of As(T), As(V) and As(III) as shown in Figure 7. Under the experimental conditions, the error limits on the prediction of the specific uptakes of As(T), As(V) and As(III) are −0.2 to +5.64%, which are within the error limits of the arsenic speciation technique as reported elsewhere.[30]

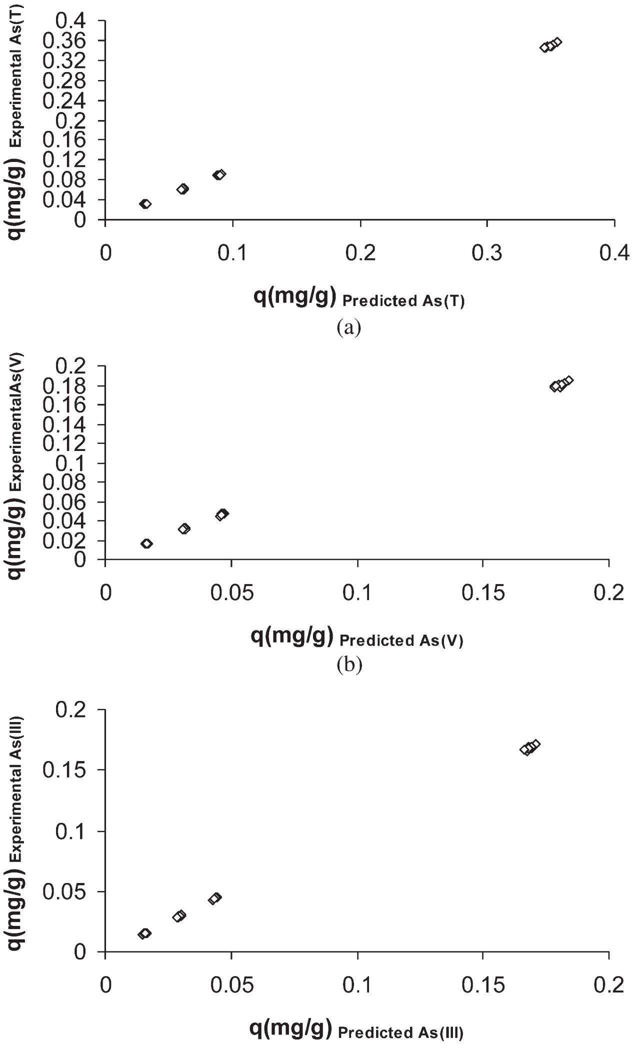

(a)

(b)

(c)

Figure 7. Predicted and experimental values of the specific uptake for the adsorption of arsenic species on GAC-Fe under varying concentration of As_o, Fe_o and Mn_o (a) for As(T), (b) for As(V), and (c) for As(III).

These equations are empirical equations, and, thus, are applicable under the domain of experimental conditions under which these are developed. Nevertheless, the methodology provides a method to compensate the effect of Fe and Mn ions in the solution on the adsorption of arsenic species on GAC-Fe surface.

Conclusions

From this work the following conclusions emerge.

1. Prediction of the nonequilibrium stage adsorption by pseudo second-order kinetic model is more accurate for all the arsenic species investigated than the other kinetic models such as pseudo first-order model, Weber and Morris model and Elovich model for this work.

2. Attachment of arsenic through the exchange of hydroxyl ions plays an important role on the kinetics of arsenic adsorption.

3. Film diffusion is the rate-determining step for the adsorption of arsenic species on GAC-Fe.

4. Polynomial isotherm provides better prediction for the specific uptake at equilibrium for all the arsenic species investigated.

5. Among the conventional isotherms, Freundlich isotherm provides better prediction for equilibrium specific uptake for all the arsenic species throughout the whole range of As_o investigated.

6. Increase in As_o Fe_o and Mn_o increases the adsorption of arsenic on GAC-Fe.

Acknowledgement

Facilities provided by IIT Roorkee and financial support provided by Ministry of Human Resource Development, Govt. of India, under grant number MHR-187-CHD is greatly acknowledged.

Literature Cited

1. Mosaferi M, Yunesian M, Dastgiri S, Mesdaghinia A, Esmailnasab N. Prevalence of skin lesions and exposure to arsenic in drinking water in Iran. *Sci Total Environ*. 2008;390:69–76.
2. Bhattacharya P, Tripathy S, Kim K, Kim SH. Arsenic fractions and enzyme activities in arsenic-contaminated soils by groundwater irrigation in West Bengal. *Ecotoxicol Environ Saf*. 2007; doi:10.1016/j.ecoenv.2007.08.015.
3. Mohan D and Pittman CU. Arsenic removal from water/wastewater using adsorbents-A critical review. *J Hazard Mater*. 2007;B142:1–53.
4. Mondal P, Majumder CB, Mohanty B. Laboratory based approaches for arsenic remediation from contaminated water: recent developments. *J Hazard Mater*. 2006;B137:464–479.
5. EPA Office of Ground water and drinking water. *Implementation guidance for the arsenic rule*. EPA report- 816-D-02–005. Cincinnati, OH; 1998.
6. WHO. *Guidelines for drinking water quality*. World Health Organisation. Geneva, Switzerland; 1993:41.
7. NHMRC. Australian Drinking Water Guidelines. National Health and Medical Council, Agriculture and Resource Management Council of Australia and New Zealand, Commonwealth of Australia, PF S93, 1996.
8. Chakraborty S, Dureja V, Bhattacharya G, Maity S, Bhattacharjee S. Removal of arsenic from ground water using low cost ferruginous manganese ore. *Water Res*. 2002;36:625–632.
9. Sarkar S, Gupta A, Biswas RK, Deb AK, Greenleaf JE, SenGupta AK. Well-head arsenic removal units in remote villages of Indian subcontinent: Field results and performance evaluation. *Water Res*. 2002;39:2196–2206.
10. Lakshmipathiraj P, Narasimhan BRV, Prabhakar S, Raju GB. Adsorption studies of arsenic on Mn-substituted iron oxyhydroxide. *J Colloid Interface Sci*. 2002;304:317–322.
11. Zaw M, Emett MT. Arsenic removal from water using advanced oxidation processes. *Toxicology Lett*. 2002;133:113–118.
12. Mondal P, Majumder CB, Mohanty B. Effects of adsorbent dose, its particle size and initial arsenic concentration on the removal of arsenic, iron and manganese from simulated ground water by Fe^{+3} impregnated activated carbon. *J Hazard Mater*. 2008;150:695–702.
13. Chen W, Parette R, Zou J, Cannon FS, Dempsey B A. Arsenic removal by iron-modified activated carbon. *Water Res*. 2007;41:1851–1858.
14. Goel R, Kapoor SK, Misra K, Sarma RK. Removal of arsenic from water by different adsorbents. *Indian J Chem Technol*. 2004;11:518–525.
15. Gu Z, Deng B, Fang J. Preparation and evaluation of GAC-based iron-containing adsorbents for arsenic removal. *Environ Sci Technol*. 2005;39:3833–3843.
16. Huang CP, Vane LM. Enhancing As^{+5} removal by a Fe^{+2} treated activated carbon. *J Water Pollut Control Fed*. 1989;61:1596–1603.

17. Vaughan R L Jr, Reed B E. Modeling As(V) removal by a iron oxide impregnated activated carbon using the surface complexation approach. *Water Res*. 2005;39:1005–1014.
18. Mondal P, Majumder CB, Mohanty B. A laboratory study for the treatment of arsenic, iron and manganese bearing ground water using Fe^{3+} impregnated activated carbon: Effects of shaking time, pH and temperature. *J Hazard Mater*. 2007a;144:420–426.
19. Lagergren S. About the theory of so called adsorption of soluble substances. *Ksver Veterskapsakad Handl*. 1898;24:16.
20. Ho YS, McKay G. Pseudo-second-order model for sorption processes. *Process Biochem*. 1999;34:451–465.
21. Weber WJ, Morris JC. Kinetics of adsorption on carbon from solution. *J Sanitary Eng Div, ASCE*. 1963;89(SA2):31–59.
22. Juang RS, Chen ML. Application of the Elovich equation to the kinetics of metal sorption with solvent impregnated resins. *Ind Eng Chem Res*. 1997;36:813–820.
23. Chien SH, Clayton WR. Application of Elovich equation to the kinetics of phosphate release and sorption in soils. *Soil Sci Soc Am J*. 1980;44(2):265–268.
24. Mondal P, Majumder CB, Mohanty B. Removal of trivalent arsenic (As(III)) from contaminated water by calcium chloride ($CaCl_2$)-impregnated rice husk carbon. *Ind Eng Chem Res*. 2007b;46:2550–2557.
25. Maity S, Chakravarty S, Bhattacharjee S, Roy BC. A study on arsenic adsorption on polymetallic sea nodule in aqueous medium. *Water Res*. 2005;39(12):2579–2590.
26. Marquardt DW. An algorithm for least-squares estimation of nonlinear parameters. *J Soc Ind Appl Math*. 1963;11:431–441.
27. Katsoyiannis IA, Zouboulis,AI. Removal of arsenic from contaminated water sources by sorption onto iron-oxide-coated polymeric materials. *Water Res*. 2002;36:5141–5155.
28. Hubbard AT.*Encyclopedia of Colloid and Surface Science*.CRC Press; 2002:3897–3898.
29. Manju GN, Raji C, Anirudhan TS. Evaluation of coconut husk carbon for the removal of arsenic from water. *Water Res*. 1998; 32(10):3062–3070.
30. Mondal P, Majumder CB, Mohanty B. Quantitative separation of As(III) and As(V) from a synthetic water solution using ion exchange column in the presence of Fe and Mn ions. *Clean-Soil Air Water*. 2007c;35:255–260.
31. Haque MN, Morrison G.M, Perrusquía G, Gutierréz M, Aguilera AF, Cano-Aguilera I, Gardea-Torresdey JL. Characteristics of arsenic adsorption to sorghum biomass. *J Hazard Mater*. 2007;14:30–35.
32. Filippova NL. Adsorption and desorption kinetics with systems having a concentration dependent coefficient of diffusion. *J Colloid Interface Sci*. 1998;203:464–476.
33. Poots VJP, McKay G, Healy JJ. J Water poll. *Cont Fed*. 1978:50; 926.
34. Allen SJ, Brown PA. Isotherm analyses for single component and multi-component metal sorption onto lignite. *J Chem Technol Biotechnol*. 1995;62:17–24.
35. Maji SK, Pal A, Pal T. Arsenic removal from real-life groundwater by adsorption on laterite soil. *J Hazard Mater*. 2008;151:811–820.
36. Michelson LD, Gideon PD, Pace EG, Katal LH. Removal of soluble mercury from wastewater by complexing techniques. *US Department of Industry: Office of Water Research Technology*. Bulletin No. 74; 1975.
37. Murugesan GS, Sathishkumar M, Swaminathan K. Arsenic removal from groundwater by pretreated waste tea fungal biomass. *Bioresour Technol*. 2006;97(3):483–487.
38. Badruzzaman M, Westerhoff P, Knappe DRU. Intra-particle diffusion and adsorption of arsenate onto granular ferric hydroxide (GFH). *Water Res*. 2004;38(18):4002–4012.
39. Thirunavukkarasu OS, Viraraghavan T, Subramanian KS, Tanjore S. Organic arsenic removal from drinking water. *Urban Water*. 2002;4(4):415–421.
40. Know KD, Kubicki JD. Molecular orbital theory study on surface complex structures of phosphates to iron hydroxides: Calculation of vibrational frequencies and adsorption energies. *Langmuir*. 2004;20: 9249–9254.
41. Fonseca MG, Oliveira MM, Arakaki LNH. Removal of cadmium, zinc, manganese and chromium cations from aqueous solution by a clay mineral. J Hazard Mate*r*. 2006;B137:288–292.
42. Lee S.*Encyclopedia of Chemical Processing*.CRC Press; 2006:45.

Manuscript received May 29, 2008, and revision received Dec. 23, 2008.